The Structure and Properties of Aluminum Alloys Produced by Mechanical Alloying: Powder Processing and Resultant Powder Structures

P. S. GILMAN AND W. D. NIX

Mechanical alloying of two aluminum alloy powders to form composite Al-Al_2O_3 powders has been studied. Changes in powder microstructure with processing are reported and interpreted. Mechanical alloying proceeds by the continual cold welding and fracturing of the constituent powder particles when subjected to the large compressive forces of a high speed mill. A suitable organic surfactant must be added so that a balance between cold welding and fracturing is obtained. The organic surfactant is embedded and finely distributed in the powder particles during mechanical alloying and is converted to discrete Al_4C_3 particles after hot pressing. The establishment of steady state processing conditions, characterized by equiaxed powder particles, a constant particle size distribution and a saturation hardness, is found to depend on the size distribution of the initial powders. The oxide particles formed and distributed during mechanical alloying are equiaxed, small (30 nm) and homogeneously distributed with a volumetric center to center distance of about 60 nm.

BEGINNING with Benjamin's successful fabrication of mechanically alloyed IN-853 in 1970,[1] several industrial laboratories concerned with the development of advanced oxide dispersion strengthened superalloys have chosen mechanical alloying as a technique for the processing of this class of alloys. While many new alloys have resulted from these material development programs, very little work on the fundamental nature of mechanical alloying has been published. The present investigation of the formation of composite Al-Al_2O_3 powder particles by mechanical alloying was conducted for the purpose of providing a better understanding of this important new process.

Mechanical alloying is a process in which constituent powder particles are repeatedly fractured and cold welded by the continuous impacting action of a milling medium. Eventually, composite powder particles, whose composition corresponds to the percentages of the respective constituents in the original charge, are formed. The resulting composite powders are characteristically dense, cohesive and homogeneous.[2]

Some dispersion strengthened aluminum alloys exhibit excellent mechanical properties at temperatures approaching their melting point. However, many of the early Al-Al_2O_3 (SAP) alloys show inconsistent mechanical behavior due to the presence of large dispersoids and heterogeneous oxide distributions. These shortcomings can be improved, but only by complicated processing and consolidation techniques such as perpendicular extrusion. Mechanical alloying circumvents many of these complicated processing steps. After powder processing by mechanical alloying, each individual powder particle should contain a fine, homogeneous oxide distribution, thus removing the need for complicated post consolidation working in order to refine and distribute the oxide dispersion.

P. S. GILMAN, formerly Graduate Research Assistant in the Department of Materials Science and Engineering at Stanford is now Research Metallurgist, INCO Research and Development Center, Inc., Sterling Forest, Suffern, NY, 10901. W. D. NIX is Professor of Materials Science and Engineering at Stanford University, Stanford, CA, 94305.

Manuscript submitted February 20, 1980.

MATERIALS AND EXPERIMENTAL PROCEDURES

Materials

Two different atomized aluminum powders were mechanically alloyed. Aluminum powder *A* is nominally 99 pct pure, while aluminum powder *B* is a preblended powder, ALCOA 601AB, which has the composition of aluminum alloy 6061. The chemical compositions of the aluminum powders are given in Table I. Powder *B* contains 1.5 pct of Nopcowax-22 DSP (ethylene bis disteramide), an organic lubricant that aids in the cold compaction of the alloy powder blend.

All powders were mechanically alloyed using a Spex No. 8000 mixer/mill. A five gram powder charge along with thirty 6.35 mm diam 52100 steel balls were loaded into a 55 ml tool steel grinding container. The mixer/mill vibrates the charged grinding container in three mutually perpendicular directions at approximately 1200 rpm. The powders were processed for the prescribed milling times without any intermediate opening of the grinding container. Between processing runs the hardened steel grinding containers were sandblasted to remove any residual cold welded material and rinsed in acetone.

Experimental Procedures

All powders were sized according to ASTM standard B214-66.[3] Two deviations from standard procedure were unavoidable. Test specimens of less than 50 grams were sized and some of the powders sieved were not granular in shape.

ISSN 0360-2133/81/0511-0813$00.75/0

Table I. Chemical Analysis of Starting and Mechanically Alloyed Aluminum Powders

	Aluminum Powder *A*		Aluminum Powder *B*	
	Starting	Mechanically Alloyed (3 h)	Starting	Mechanically Alloyed (3 h)
Al	99	97.45	96	95
Al_2O_3	0.446 (.35)	1.27 (1.01)	0.3 (.23)	1.98 (1.58)
C	—	1.14 (1.36)	—	1.08 (1.29)
Mg	—	<0.005	1.0	0.81
Si	0.15	0.02	0.67	0.61
Cu	0.02	<0.01	0.25	0.22
Fe	0.34	0.11	0.145	0.13
Nopcowax-22		—	1.5	—
Other	balance	balance	balance	balance

*wt pct (Vol pct)

Powder particle microhardness measurements were restricted to the −80 to +100 mesh powders (150 μm to 180 μm) in order to insure consistency and reproducibility in the hardness measurements.

To observe the morphology of processed aluminum powders by scanning electron microscopy, powder specimens were prepared by affixing a small amount of powder to an aluminum specimen stud with double stick tape. A thin layer of gold was subsequently vapor deposited over the powders to assure uniform conductivity.

A special specimen mounting technique was utilized to observe the microstructures of individual mechanically alloyed powders. The particular aluminum powders were mixed with refined bakelite powder and the entire mixture was consolidated in the usual pressure sintering manner. The cylindrical aluminum-bakelite compact was sectioned through the cylinder axis exposing sectioned powder particles that could be prepared by standard metallographic procedures. All sectioned powder particles were etched with modified Kellar's reagent.

To analyze the oxide distribution developed by mechanical alloying, the processed powders were vacuum hot pressed so that thin foils could be prepared for transmission electron microscopy. Additional microstructural refinement by subsequent deformation processing, *i.e.*, extrusion or rolling, was purposely avoided. The powders were vacuum hot pressed to reduce the possibility of hydrogen gas induced porosity. Prior to vacuum hot pressing, all aluminum powders were cold compacted under a pressure of 690 MPA (100 ksi) to a green density of approximately 2.15 g/cm.[3] All aluminum powders were vacuum hot pressed at 773 K at pressures up to 327 MPA (47 ksi) following the techniques reported by Bloch[4] and Hansen.[5]

Consolidated aluminum samples were etched and anodized using Barker's reagent for analysis by polarized light microscopy.

All transmission electron microscopy specimens were prepared from sections taken perpendicular to the hot pressing direction. Samples were jet polished at 6.5 V in an 80 vol pct ethanol −20 vol pct perchloric acid solution cooled to 258 K.

EXPERIMENTAL RESULTS

Mechanical Alloying of Aluminum Powder B

The mechanical alloying of aluminum powders can be followed by observing the microstructural changes that occur with increased milling time. The powder morphologies and microstructures for powder *B* processed into various stages of mechanical alloying are shown in Fig. 1. The atomized powder *B* contains a wide distribution of powder sizes as shown in Fig. 2. The fine dendritic structure of the powder particles is difficult to resolve optically (Fig. 1(*a*)). At 10 min into the process (Fig. 1(*b*)) cold welded composite particles are clearly evident. The cold welded lamellae are parallel to each other even though the particles themselves are heavily distorted. The cold welded bond between adjacent lamellae does not appear to be complete, as spaces between the cold welded layers can be seen, With time the cold welding becomes more extensive and the composite particles are denser.

The variation in microhardness with processing time is shown in Fig. 3. A slight drop in the powder particle microhardness is observed in the early stages of mechanical alloying. Benjamin and Volin[6] also observed a hardness minimum after short processing times during the mechanical alloying of an Fe-Cr alloy. The hardness drop is due to the incomplete cold welding of the flaked particles during the early stages of mechanical alloying. The structure behaves in a spongy fashion and exhibits a low hardness. After 10 min of processing, the parallel lamellae are separated in some regions, but after 20 min of processing the layers are welded together and the powder particles appear fully dense. At this stage most of the particles have been severely deformed and cold worked, as reflected by the increased hardness over the starting powders.

Both the large and small particles are equiaxed after 1 h of processing (Fig. 1(*c*)). Compared to earlier stages of mechanical alloying, there is a sharp decrease in the number of coarse, flake-like powders, which are transformed to equiaxed particles by the fragmentation of their extremities. The fragmented particles may or may not subsequently reweld. The

fine composite particles consist of the composite fragments of the larger powder particles. A rapid increase in microhardness to about 120 VH is measured after one hour of processing time.

The progress of mechanical alloying is clearly illustrated by the presence of small equiaxed composite particles. These particles must be produced by the continuous cold welding and fracturing of the aluminum powder.

The fine lamellar microstructure can no longer be resolved in the equiaxed speroidal particles present after 3 h of mechanical alloying (Fig. 1(*d*)). From this microstructural observation and the knowledge that the aluminum particles have repeatedly cold welded

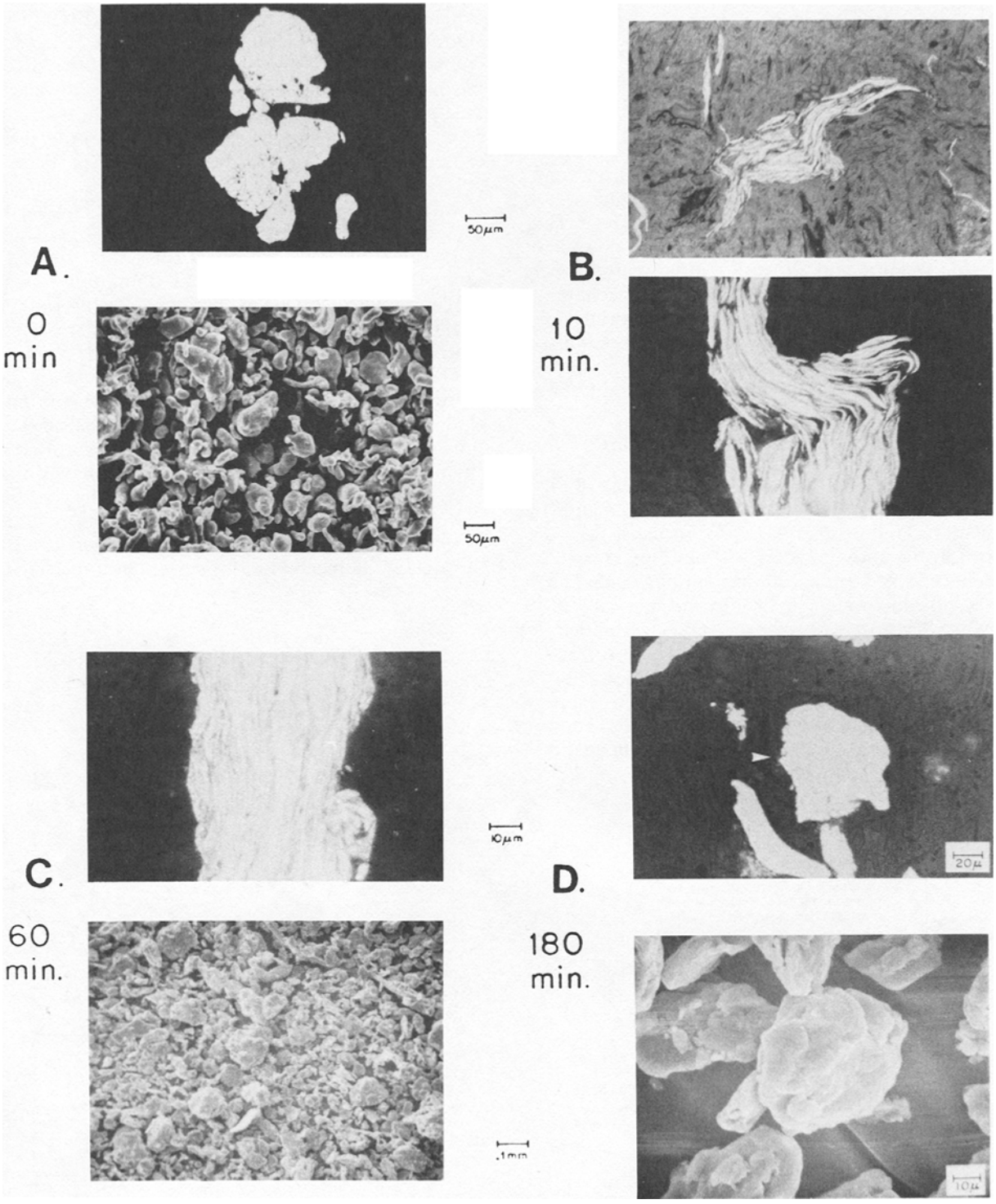

Fig. 1—Microstructures and morphologies of Alcoa 601 AB (alloy *B*) powder after mechanical alloying for various times. The composite structures of large powders are shown in the optical micrographs while the powder morphologies can be seen in the scanning electron micrographs.

and fractured, it may be concluded that the powders are fully mechanically alloyed. Employing the criteria suggested by Benjamin and Volin,[6] it is further concluded that mechanical alloying has reached a steady state, because the powder particle size distribution stays constant with increased milling time and a saturation hardness, 160 VH, has been attained.

Mechanical Alloying of Aluminum Powder A

In the early stages of this work it was learned that pure aluminum *A* powders cannot be mechanically alloyed because the process is impeded by the excessive cold welding of the powders (see Fig. 4). Excessive cold welding prevents the particles from fracturing and thus the system does not achieve the critical balance between cold welding and fracturing that is necessary for successsful mechanical alloying.

It was postulated that the presence of 1.5 wt pct Nopcowax-22 DSP, an organic lubricant in powder *B* delays cold welding and allows the aluminum powder particles to work harden and fracture. To mechanically comminute aluminum powders, appropriate surfactants, usually in the form of organic waxes, must be added to the powders prior to processing to prevent excessive cold welding. The original producers of SAP relied on organic waxes such as Nopcowax-22, sterotex or acrawax[7] to mill aluminum powders into flaked particles.[5]

A small amount of *B* powder was heated at 789 K for 10 h in order to remove the Nopcowax-22 DSP by vaporization. Upon subsequent processing in the shaker mill, the alloy powders without Nopcowax-22 DSP behaved like the pure aluminum powders. The annealed powders were successfully mechanically alloyed when 2 wt pct Nopcowax-22 DSP was added prior to processing. Finally, when a suitable surfactant was added to the pure aluminum powder, the powders could easily be mechanically alloyed. Thus, successful mechanical alloying of aluminum at room temperature requires the presence of a surfactant to prevent excessive cold welding.

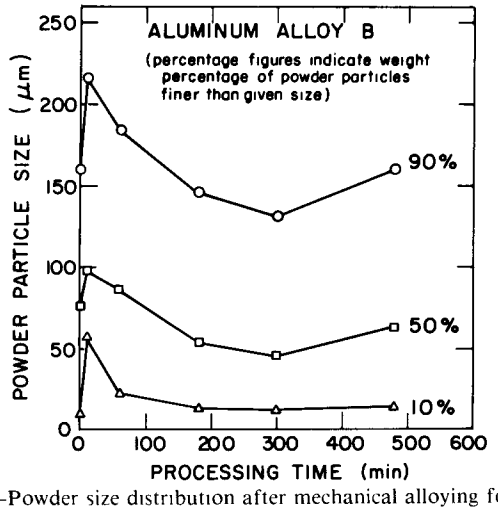

Fig. 2—Powder size distribution after mechanical alloying for various times (aluminum alloy *B*).

Volin[2] has previously reported the importance of the addition of surfactants or process control agents for the mechanical alloying of certain nickel base alloys that do not contain oxide dispersions, and Benjamin and Bomford[8] also found it necessary to add certain organics to the initial powder charges to successfully mechanically alloy dispersion strengthened aluminum.

The mechanical alloying of aluminum *A* with Nopcowax-22 DSP is illustrated in Fig. 5. Cold welding is evident in powders processed for 5 min (FIG. 5(*b*)). Both the small and large powder particles become equiaxed after 1 h of processing and a convoluted lamellar structure characterizes the larger powder particles (Fig. 5(*c*)). Finally, after 2 h of processing, the prior particles are barely resolvable with optical microscopy and the large equiaxed powder particles have a definite composite appearance. However, the small powder particles appear flat and are not equiaxed. The entire powder charge is not as uniformly equiaxed as the alloy powders processed for similar times. At processing times greater than 2 h aluminum powder *A* porcessed with Nopcowax-22 appears to be fully mechanically alloyed, even though the powder particle morphologies are not uniformly equiaxed.

The powder size distribution of mechanically alloyed *A* powders with Nopcowax-22 DSP continually changes with time as shown in Fig. 6. A steady-state size distribution does not develop as in the mechanical alloying of the *B* powders. As shown in Fig. 3, the microhardness of the powder particles also fluctuates about a value of 130 VH. It should be remembered that 94 pct of the starting *A* powders can pass through a 325 mech (45 μm) sieve. Once mechanical

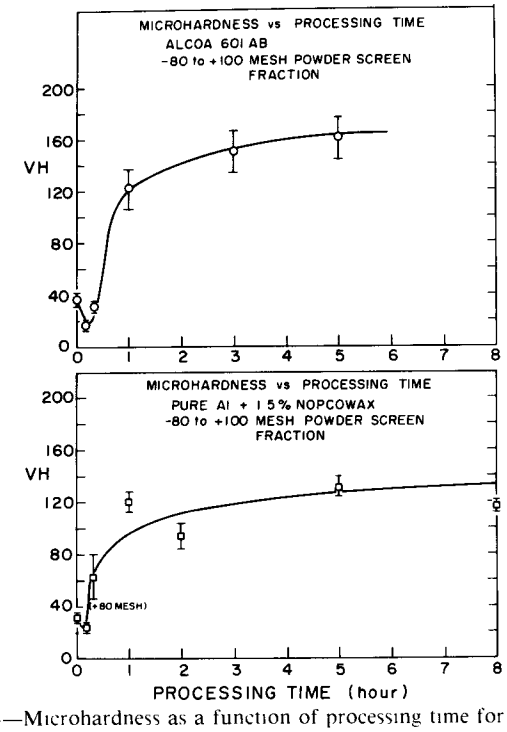

Fig. 3—Microhardness as a function of processing time for Alcoa 601 AB (alloy *B*) powders (upper graph), and Pure Al + 1.5 pct Nopcowax-22 (alloy *A*) powders (lower graph).

alloying begins these small particles must flatten and cold weld before there is simultaneous milling of large and small particles. By the time a broad powder size distribution is reached much of the Nopcowax-22 DSP has been trapped between the cold welded layers of the composite particles, thus decreasing the amount of surfactant available to delay cold welding. The narrow starting powder size distribution makes it more difficult to reach the steady state processing conditions. Nevertheless, metallographic analysis shows that the powders have been successfully mechanically alloyed.

Chemical Analysis

The chemical compositions of *A* powders with 1.5 wt pct Nopcowax-22 DSP and *B* powders mechanically alloyed for 3 h, *MA-A* and *MA-B* respectively, are given in Table I. The carbon contents of *MA-A* and *MA-B* are 1.08 and 1.14 vol pct, respectively. These carbon concentrations result from the residual Nopcowax-22 DSP remaining in both powders. During mechanical alloying the surfactant is entrapped between the cold welded lamellae of the composite particles, in contrast to the case of conventional ball milling wherein the surfactant remains on the surface of the powder paricles and can be easily leached or burned away. The amount of carbon detected in each powder is equivalent to the amount of carbon added in the form of 1.5 wt pct Nopcowax-22 DSP (C_2H_2-2($C_{18}H_{36}ON$)).

The amounts of iron in the processed aluminum powders are below the compositional limits given for the starting powders. Contamination of the mechanically alloyed aluminum powders from the tool steel grinding container and the 52100 steel balls is therefore not a problem. The elaborate techniques used to prevent contamination during the mechanical alloying of some nickel,[9] cobalt,[10] and iron[11] ODS alloys are not necessary for the mechanical alloying of aluminum.

The oxide content of the mechanically alloyed aluminum powders as a function of processing time is shown in Fig. 7. As measured by inert gas fusion, all of the oxygen was assumed to be combined with aluminum as Al_2O_3. The entrapped oxygen in the hardened tool steel grinding container can form only 0.59 wt pct or 0.47 vol pct Al_2O_3. After 10 min of processing the aluminum powders contain more oxygen than is available in the sealed grinding container. The additional oxygen pick-up occurs when the grinding can is opened to the atmosphere after processing and freshly fractured and flattened surfaces of the aluminum particles oxidize. The variance in the oxide content of MA-A powders reflects the changes in the powder particle size distribution with processing time.

Thermal Response

Differential thermal analysis (DTA) was employed to study the homogeneity of *MA-B* powders. When heated the as-atomized *B* powders begin to melt at 888 K. This is indicated as point "A" on the DTA curve in Fig. 8, and corresponds to the solidus temperature for the ternary Al-Mg-Si system at the composition of the *B* powder. The powders are completely melted at 943 K, point "B". The melting curve is characteristic of a single phase material and is expected from the atomized aluminum powders.

The melt supercools slightly on freezing and begins

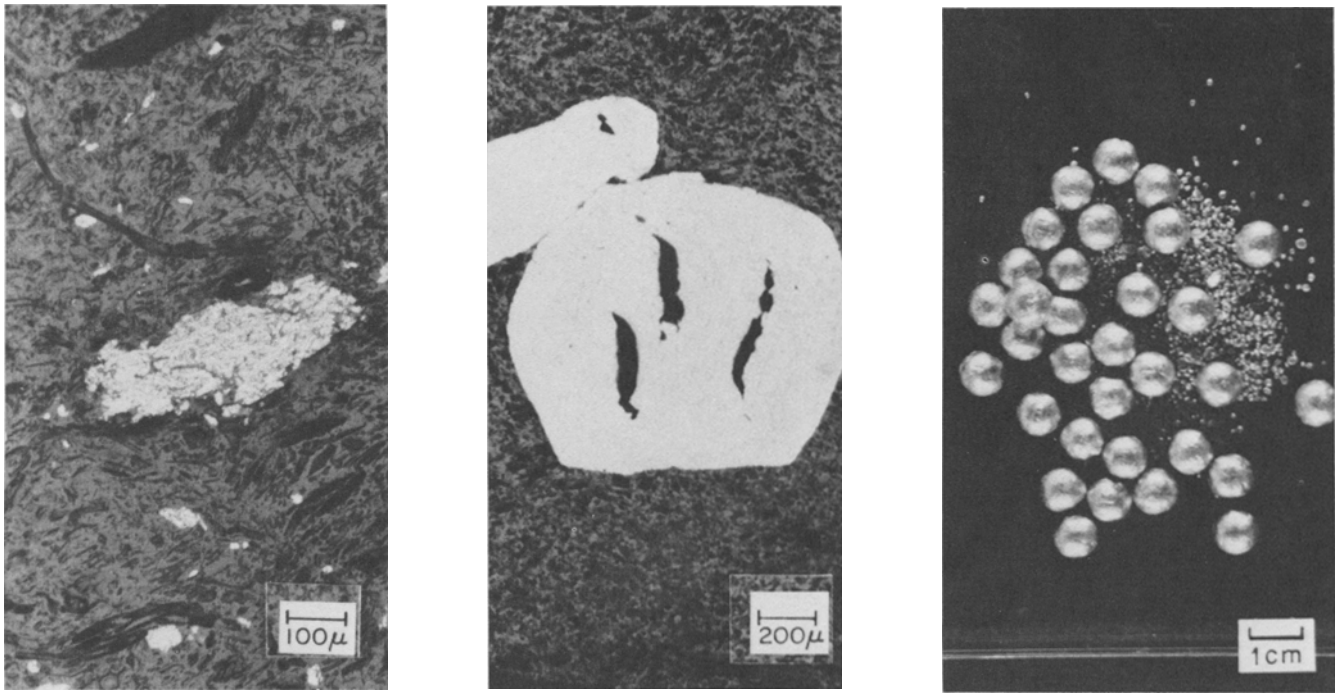

(a) *(b)* *(c)*

Fig. 4—Aluminim alloy *A* powders (99 pct Al) processed for various times. (*a*) Two minutes, (*b*) and (*c*) twenty minutes.

to solidify at 898 K, point "C". Before the liquid completely solidifies, a new reaction commences at 818 K, point "D". This corresponds to the (Al)-Mg_2Si-(Si) eutectic that forms at 832 K. The eutectic contains 4.6 wt pct Al.[12] Due to non-equilibrium freezing, there is segregation in the melt and the last material to solidify is of the eutectic composition.

MA-B powders exhibit the same thermal behavior as unprocessed alloy powders on melting, as seen in the curve from "F" to "G". However, upon freezing there is no macrosegregation in the melt as the thermal response of the alloy on freezing is that of a single phase material, as seen in the curve from "H" to "I". Although not shown, repeated melting and freezing of the mechanically alloyed powders produce DTA curves which are the same as those for initial melting and freezing. After mechanical alloying, the alloy powders are internally homogeneous and the fine oxide distribution in the particles inhibits any segregation or coring in the melt.

To investigate the chemical homogeneity of mechanically alloyed powders, a small amount of *B* powder was heated for 10 h at 789 K in the solution treating temperature range for these alloy powders, and air cooled. The objective of this heat treatment was to precipitate Mg_2Si in the *B* powder such that on subsequent heating the dissolution of Mg_2Si could be

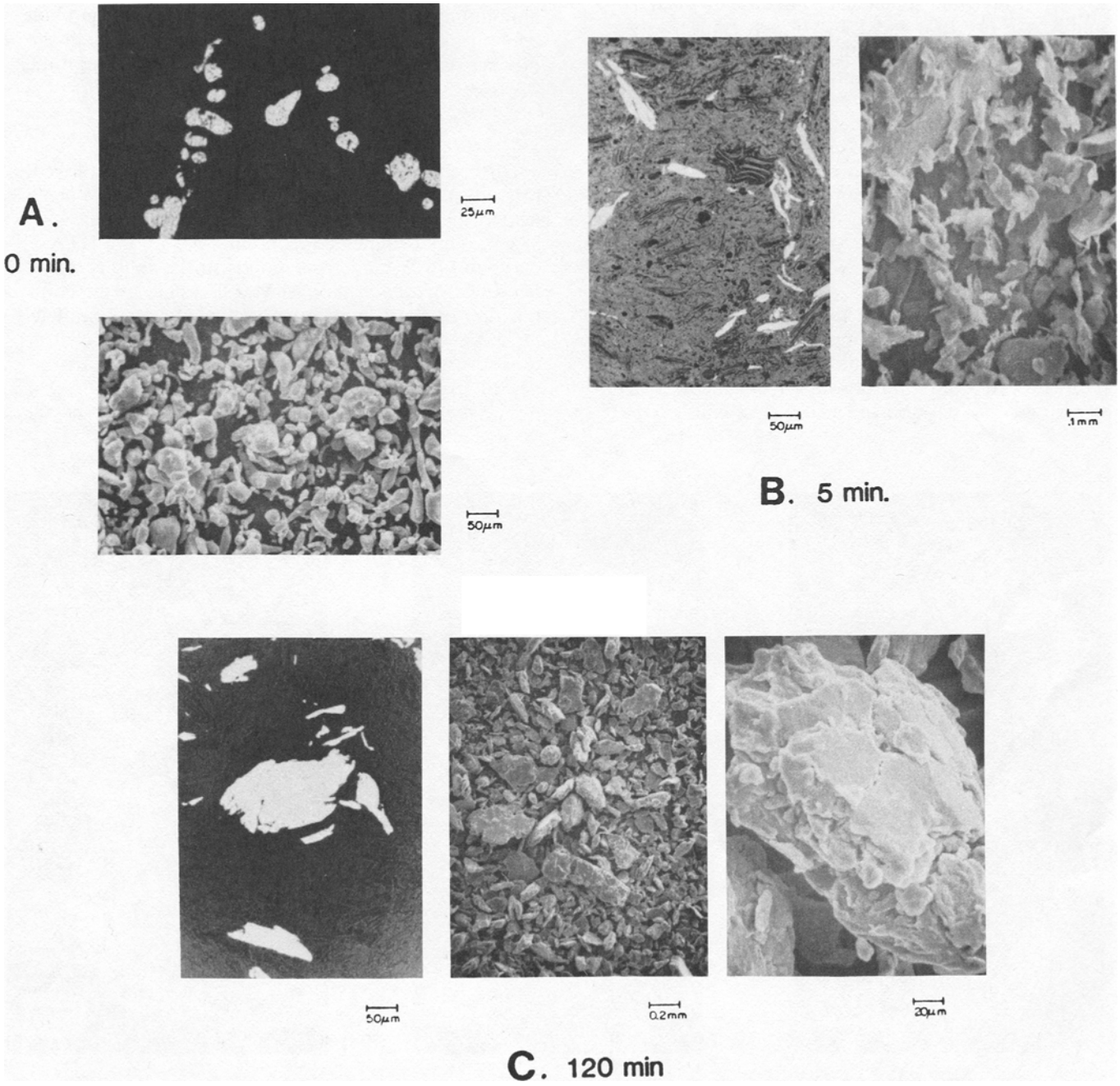

Fig. 5—Microstructures and Morphologies of aluminum alloy *A* mechanically alloyed with Nopcowax-22 DS for various times.

monitored by DTA. On heating, the dissolution of Mg_2Si appears as a bump on the DTA curve, as shown by point "A" in Fig. 9. The material behaves as before on cooling as the melt segregates and the last material to solidify is of the ternary eutectic composition. Also shown in Fig. 9 is the thermal response of the specially heat treated powders mechanically alloyed for 3 h (surfactant added before processing). Again the response is that of a chemically homogeneous single phase material. This suggests that mechanical alloying breaks up and finely distributes the Mg_2Si formed during the previous annealing treatment.

The Structure of Consolidated Material

The mechanically alloyed aluminum powders were too hard to uniaxially cold compact to green densities greater than 80 pct of theoretical density. This is due to the severe cold working of the powder particles during processing. However, near theoretical densities were successfully achieved by vacuum hot pressing. The hardness of the various vacuum hot pressed alloys are given in Table II. The increased hardness of the mechanically alloyed materials indicates that much of the cold work produced by mechanical alloying remains after hot pressing.

Mechanically alloyed pure aluminum (*MA-A*) is unrecrystallized after vacuum hot pressing. As shown in Fig. 10, prior particle boundaries are clearly evident

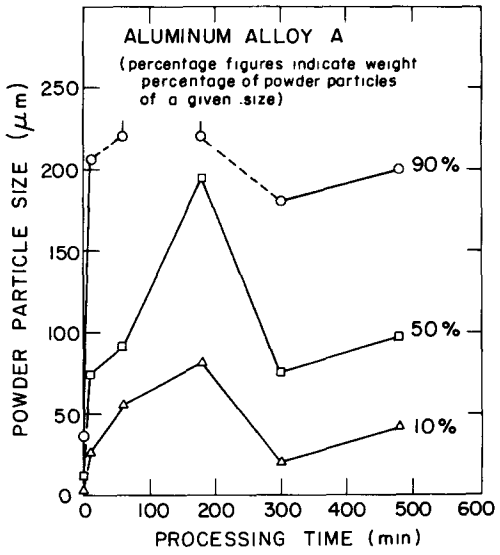

Fig. 6—Powder size distribution after mechanical alloying for various times (aluminum alloy *A*).

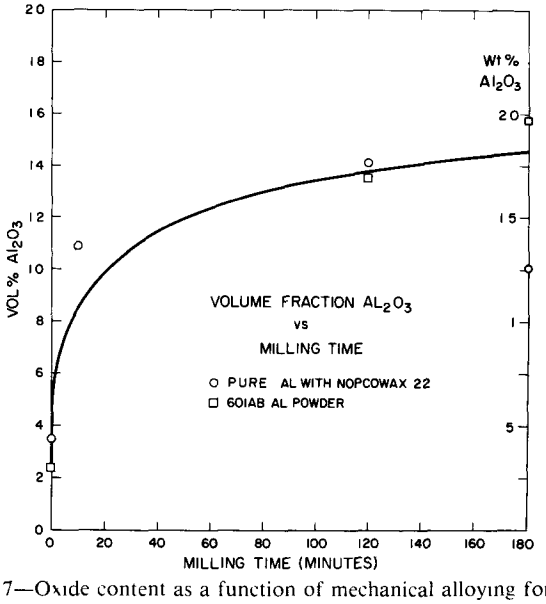

Fig. 7—Oxide content as a function of mechanical alloying for aluminum alloys.

Table II. Hardness of Vacuum Hot Pressed Aluminum Alloys

	Aluminum Powder *A**	Aluminum Powder *B*
Starting powders	18.3 R_F	12 R_F
Mechanically alloyed (3 h)	56.4 R_B	74.1 R_B

*Containing 1.7 pct Nopcowax 22 DS.

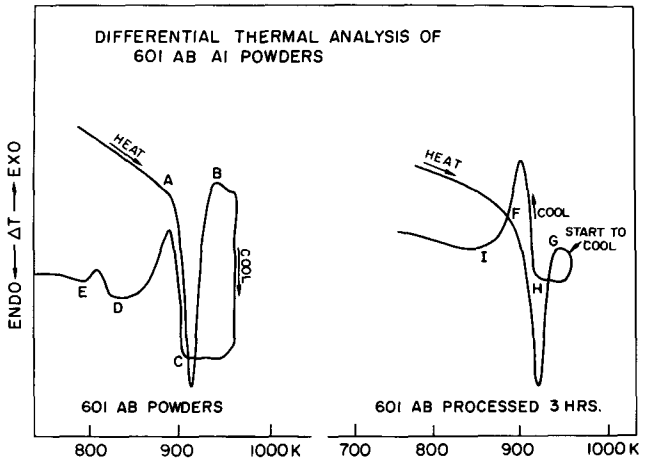

Fig. 8—Differential thermal analysis for aluminum alloy *B* (Alcoa 601 AB) powders before and after mechanical alloying.

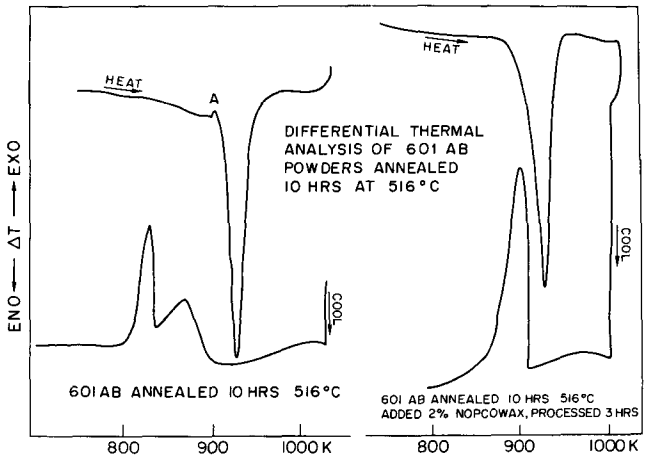

Fig. 9—Differential thermal analysis for aluminum alloy *B* (Alcoa 601 AB) powders previously annealed at 789 K for 10 h and air cooled, before and after mechanical alloying.

in the microstructure of this material. Also the microstructure shows some subgrains approximately 0.3 μm in diam.

The uniformed distribution of Al_2O_3 formed during the mechanical alloying of pure aluminum *A* powders with Nopcowax-22 DSP can be seen in Fig. 11. The average planar diameter of the oxide particles is 30 nm and the center to center spacing between nearest neighbor particles is 60 nm.

A closer look at the electron diffraction pattern of *MA-A* reveals the existence of aluminum carbide (Al_4C_3). The aluminum carbide is in the form of small

Fig. 10—The grain structure of mechanically alloyed aluminum alloy *A* after vacuum hot pressing at 773 K and 207 MPa (30 ksi).

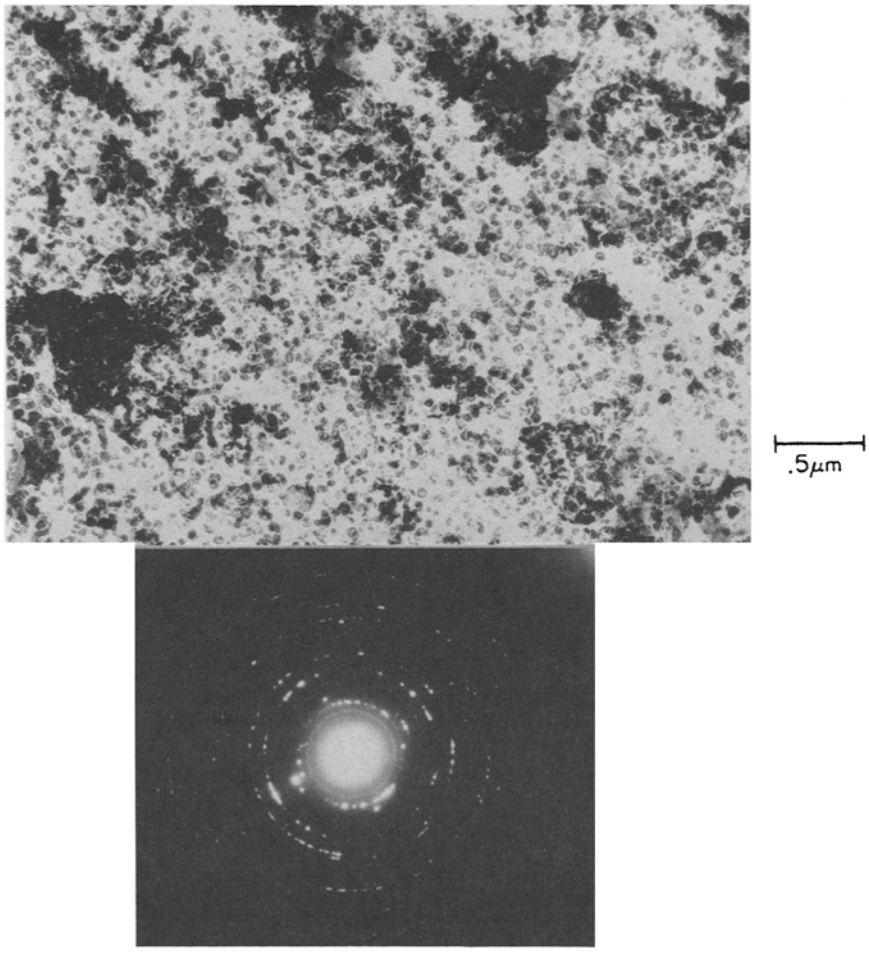

Fig. 11—The dispersoid structure of mechanically alloyed alloy *A* after vacuum hot pressing at 773 K and 207 MPa (30 ksi). The electron diffraction pattern indicates the presence of γ-Al_2O_3.

spherical particles and is clearly evident in the high magnification dark field electron micrograph, Fig. 12. The Al_4C_3 particles have an average diameter of 7.7 nm and a point to point spacing of 42 nm.

The *MA-B* powders recrystallize during vacuum hot pressing, as shown in Fig. 13. The microstructure of this material is similar to the microstructure of wrought aluminum alloy 6061 T-6 which has been worked into rod form, annealed and aged.

The oxide distribution developed in *MA-B* aluminum powder is quite uniform (Fig. 14). The oxide particles (for example at a point A of Fig. 14) are equiaxed, approximately 30 nm in diam and have a point to point particle spacing of 60 nm. The very small particles present (for example at point B) are Al_4C_3, as indicated by electron diffraction. The Al_4C_3 particles are 26 nm in diam and have a point to point spacing of 86 nm. The darker particles at C, which are approximately the same size as the Al_2O_3 dispersoids, are the magnesium silicide (Mg_2Si) precipitates formed during the slow cooling of the vacuum hot pressed compact. The Mg_2Si particles are approximately 33 nm in diam and have a center to center spacing of 56 nm.

The blocky, lightly shaded areas located throughout the vacuum hot pressed *MA-B* microstructure, for example at D of Fig. 14, are voids. This was verified using the defocus contrast technique described by Lloyd and Nakahara.[13] This indicates that the vacuum conditions were not adequate to successfully hot press *MA-B* powders. Vacuum hot pressed *MA-B* aluminum could easily be warm rolled at 498 K to a 75 pct reduction in thickness. Warm rolling produced only minimal amounts of edge cracking. However, the blocky voids are not removed by this thermomechanical treatment.

The unrecrystallized mechanically alloyed pure aluminum (*MA-A*) could not be successfully warm rolled at 498 K but could be hydrostatically extruded to a reduction of area of 64 pct at ambient temperature. The difficulty in working *MA-A* is due to the highly worked structure that remains even after hot pressing.

DISCUSSION

The oxide dispersoids that are uniformly distributed in mechanically alloyed aluminum are equiaxed, and almost spherical in shape. These oxides were generated from two sources, the aluminum oxide film that covers the surface of an original aluminum powder particle and the oxide generated by the oxidation of freshly flaked or fractured particles surfaces exposed during mechanical alloying. Mechanical alloying breaks up and continuously embeds these oxides into the matrix of the composite aluminum powders by the repeated fracturing and cold welding of the powder charge. Eventually each individual powder particle contains a homogeneous oxide distribution.

The structural parameters of the oxide dispersion in mechanically alloyed Al-Al_2O_3 are compared to those for conventional Al-Al_2O_3 products, fabricated and

Fig. 12—Dark field electron micrograph of mechanically alloyed alloy *A* after vacuum hot pressing. The Al_4C_3 particles appear as white spots.

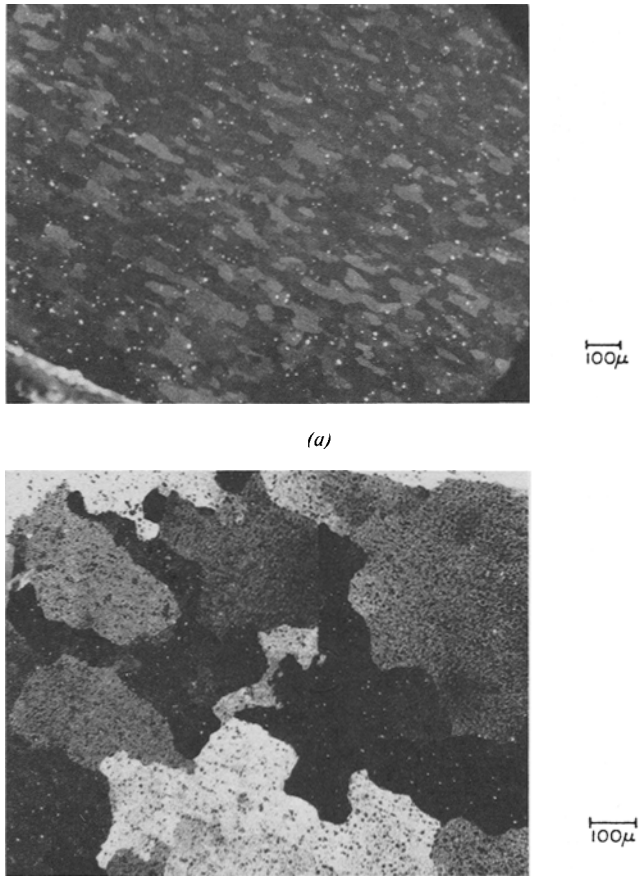

(a)

(b)

Fig. 13—A comparision of the grain structures of (*a*) 6061 Aluminum in the T-6 condition and (*b*) mechanically alloyed and vacuum hot pressed alloy *B* (Alcoa 601 B).

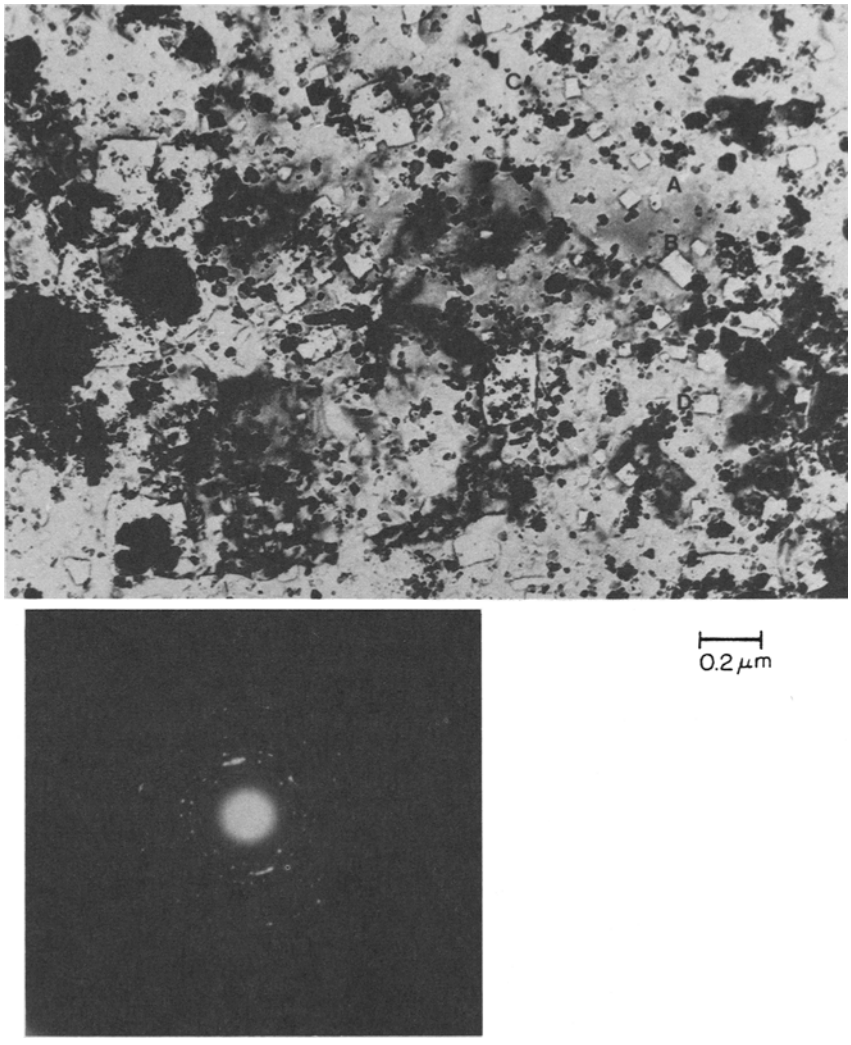

Fig. 14—Mechanically alloyed alloy *B* after vacuum hot pressing. Various second phase particles are: (A) Al_2O_3 dispersoids, (B) Al_4C_3 dispersoids, (C) Mg_2Si precipitates, and (D) gas generated voids.

Table III. Structural Parameters for Various Al-Al_2O_3 Alloys

Alloy	Raw Material	Al_2O_3 Content, (vol pct)	Average of Oxide Particles, nm	Surface to Surface of Oxide Particles, nm
Aluminum Powder *A* (pure aluminum)	Atomized Powder + Mechanical Alloying	1.01	30.3	30.7
Aluminum Powder *B* (ALCOA 601AB)	Atomized Powder + Mechanical Alloying	1.58	33	24.7
MA Al (Benjamin & Bomford)	Atomized Powder + Mechanical Alloying	2.51 – 4.20	30†	30†
Al MD 13	Atomized Powder	0.19 ± 0.03	47	740
Al MD 201	Atomized Powder	0.45 ± 0.04	36	360
Al MD105	Atomized Powder	0.79 ± 0.04	32	240
Al R 400	Atomized Powder	0.92 ± 0.05	27	180
SAP-ISML 960	Flake Powder	3.8 ± 0.2	46	130
SAP 930	Flake Powder	6.8	53	104
SAP-ISML 895	Flake Powder	8.1	57	98
SAP ISML	Flake Powder	11.6	63	83
Al MD 201-OX	Atomized	1 ± 0.2	74	480
Al MD 201-OX	High Temperature	3 ± 0.2	120	400
Al MD 105-OX	Oxidized	1.7 ± 0.2	44	210
Al MD 105-OX	Oxidized	2.9 ± 1.9	69	240

*For MA materials diameter of equiaxed oxides; for other materials, diameter of equivalent spheres.
†Assumed to be similar to other MA Al alloys.

reported by Hansen,[14,15] in Table III. The conventional Al-Al_2O_3 products were consolidated by a hot pressing technique similar to the one used to consolidate the mechanically alloyed materials. Also, the conventional Al-Al_2O_3 products were doubly hot extruded in mutually perpendicular directions in order to insure a uniform distribution of the platelet shaped oxide particles. Clearly, the oxide dispersions in the mechanically alloyed aluminum alloys are superior to those of the conventional Al-Al_2O_3 alloys that have been doubly extruded. Not only do the oxide particles in mechanically alloyed aluminum alloys have a similar diameter, but they are also more equiaxed, uniform and homogeneously distributed.

The Al_4C_3 dispersoids observed in the mechanically alloyed aluminum alloys have a rhombohedral crystal structure and they are formed from the residual lubricant, Nopcowax-22 DSP, that has been dispersed throughout the aluminum composite particles during mechanically alloying. Upon vacuum hot pressing at 773 K, the Nopcowax-22 DS is reduced by the aluminum, thus yielding aluminum carbide, nitrogen, oxygen and hydrogen. The oxygen may combine with the aluminum to form additional Al_2O_3, while the nitrogen and hydrogen are removed during vacuum hot pressing. Al_4C_3 dispersoids have been previously found to form in aluminum composite materials subjected to temperatures above 773 K.[16] They have also been found in SAP alloys heated above 873 K, as a by-product of the organic material used as a surfactant and vehicle during ball milling.[17] Previously, Al-Al_4C_3 dispersion strengthened systems have been fabricated by conventional milling[18] and by mechanical alloying.[19]

The blocky shaped voids present in the matrix of the vacuum hot pressed, mechanically alloyed 601AB aluminum (*MA-B*) are the result of water vapor and hydrogen gas generation during the vacuum hot pressing operation. Hydrogen gas is known to produce gas holes in SAP materials when heated above 673 K.[20] Also, the successful sintering of cold compacted 601AB alumimum can only be accomplished in a very dry atmosphere.[21]

Mechanically alloyed pure aluminum does not recrystallize on vacuum hot pressing because the oxide dispersoid acts to inhibit recrystallization. This is consistent with previous findings that recrystallization is inhibited in Al-Al_2O_3 alloys containing small ($< 1\ \mu m$ in diam) closely spaced ($< 0.5\ \mu m$ spacing) particles.[22-24]

MA-B recrystallizes on hot pressing because this material is able to work harden more than pure aluminum during mechanical alloying. *MA-B* powder has a microhardness of 160 VH as compared to 130 VH for processed pure aluminum. This high degree of cold working may reduce the critical size of the recrystallization nucleus; therefore the retarding effect of the dispersed phase during nucleation may be reduced or completely removed. Hansen and Bay[23] found that Al-0.6 wt pct Al_2O_3 cold drawn 50 pct could not be recrystallized. However, after 80 or 90 pct reduction there is little retardation in the recrystallization kinetics and this material recrystallizes.

SUMMARY AND CONCLUSIONS

Mechanical alloying to produce Al-Al_2O_3 composite powders has been shown to be a viable and technologically significant process. During the mechanical alloying process the starting aluminum powders are subjected to very large compressive forces that flake and eventually fracture the aluminum particles, exposing fresh surfaces of aluminum to be oxidized. As processing continues, the aluminum powders are repeatedly cold welded to each other and fractured causing a continual refinement and homogenization of the oxide dispersion. When the mechanical alloying is complete the Al_2O_3 dispersoids are very small, approximately 30 nm in diam, equiaxed and homogeneously dispersed throughout the aluminum matrix. The oxide particles have a volumetric center to center distance of 60 nm.

The significant results are:

1) A suitable surfactant, such as Nopcowax-22 DSP is necessary to successfully mechanically alloy aluminum. Aluminum easily cold welds thus a surfactant must be added to the starting powders to achieve a balance between cold welding and particle fracture.

2) Residual surfactants become embedded and finely distributed throughout the composite mechanically alloyed powder. After hot pressing the residual organic surfactant is converted to Al_4C_3.

3) The achievement of a steady-state processing condition, *i.e.*, equiaxed powder particles, constant powder size distribution and a saturation hardness, signifying the completion of mechanical alloying, depends on the initial size distribution of the powders to be mechanically alloyed.

ACKNOWLEDGMENTS

The authors wish to thank their colleagues at Stanford University for their contributions to this research. The work was supported by the Air Force Office of Scientific Research under Grant 77-3128 A-B. The preparation of this paper was supported in part through an Industrial Fellowship granted to P. S. Gilman by the Brown-Boveri Research Centre, Brown-Boveri and Company, Baden-Dättwil, Switzerland.

REFERENCES

1. J. S. Benjamin: *Met. Trans.*, 1970, vol. 1, p. 2943.
2. T. E. Volin: U. S. Patent No. 3,877,930 (Apr. 15, 1975).
3. ASTM Standard B 214-66.
4. E. A. Bloch: *Metall. Rev.*, 1961, vol. 6, p. 193.
5. N. Hansen: *Powder Met.*, 1967, vol. 10, p. 94.
6. J. S. Benjamin and T. E. Volin: *Met. Trans.*, 1974, vol. 5, p. 1929.
7. H. Hausner: *Handbook of Powder Met.*, p. 331, Chem. Pub. Co., Inc., 1973.
8. J. S. Benjamin and M. J. Bomford: *Met. Trans. A*, 1977, vol. 8A, p. 1301.
9. G. H. Gessinger: *Met. Trans. A*, 1976, vol. 7A, p. 1203.
10. D. L. Klarstrom and R. Grierson: Air Force Materials Laboratory Technical Report, TR-74-34, March (1974).
11. I. G. Wright and B. A. Wilcox: *Met. Trans.*, 1974, vol. 5, p. 957.
12. L. H. Willey: *Metals Handbook*, 8th ed., 1973, vol. 8, p. 396.
13. J. R. Lloyd and S. Nakahara: *J. Vac. Sci. Technol.*, 1977, vol. 14, p. 655.

14. N. Hansen: *J. Nucl. Mater.*, 1972, vol. 43, p. 339.
15. N. Hansen: *Acta Met.*, 1976, vol. 18, p. 1376.
16. G. Blankenburgs: *J. Aust. Inst. Met.*, 1969, vol. 14, p. 236.
17. G. L. Copeland, M. M. Martin, D. G. Harman, and W. R. Martin: *Powder Technol.*, 1969/1970, vol. 3, p. 136.
18. A Berndorf: French Patent Applic., 2,239,535 (Feb. 28, 1973); Austrian, 6779/73 (Aug. 2, 1973).
19. G. Jangg, F. Kutner, and G. Korb: *Powder Met. Int.*, 1977, vol. 9, p. 24.
20. N. Hansen, B. Kindl, and E. Adolph: *Les Mem. Sci. Rev. Met.*, 1963, vol. 60, p. 285.
21. J. H. Dudas and W. A. Dean: *Int. J. Powder Met.*, 1969, vol. 5, p. 21.
22. E. J. Westerman and F. V. Lenel: *Trans. TMS-AIME*, 1960, vol. 218, p. 1010.
23. D. Nobili and R. De Maria: *J. Nucl. Mater.*, 1965, vol. 17, p. 5.
24. N. Hansen and B. Bay: *J. Mater. Sci.*, 1972, vol. 7, p. 1351.